Carboxylic Acid-Terminated Hyperbranched Polybenzoxazole and Its Polyarm-Star Block Copolymers

Jong-Kwan Lim,[†] In-Yup Jeon,[†] Christopher B. Lyons,[‡] Michael C. Laufersweiler,[‡] Loon-Seng Tan,*[,§] and Jong-Beom Baek*[,†]

Ulsan National Institute of Science and Technology (UNIST), Ulsan 689-805, South Korea; Southwestern Ohio Council for Higher Education, Miami Valley Research Park, Dayton, Ohio 45420-4015; and Nanostructured & Biological Materials Branch, Materials & Manufacturing Directorate, Air Force Research Laboratory, AFRL/RXBN, Wright-Patterson Air Force Base, Dayton, Ohio 45433-7750

Received October 25, 2008; Revised Manuscript Received January 2, 2009

ABSTRACT: A new AB_2 monomer, 5-amino-4-hydroxyisophthalic acid hydrochloride, was synthesized and polymerized in poly(phosphoric acid) (PPA) to afford a carboxylic acid-terminated hyperbranched polybenzoxazole (HPBO). Taking advantage of the large number of peripheral carboxylic acid groups on HPBO, polyarm-star block copolymers, HPBO-*b*-*m*PEK and HPBO-*b*-*p*PEK, were conveniently prepared in the same reaction medium with additional amounts of phosphorus pentoxide (P_2O_5) via "direct" Friedel−Crafts acylation reaction with 3- and 4-phenoxybenzoic acids as AB monomers. All the resulting polymers displayed polyelectrolyte behaviors in solution due to the large number of carboxylic acid termini. The UV−vis absorption intensities, which increased as polymer concentration was increased, showed quasi-linear dependence in all sample solutions. The emission intensity drastically decreased as the concentration of HPBO core polymer was increased, while the block copolymers were not much affected by concentration variation. The emission behaviors of HPBO-*b*-*m*PEK and HPBO-*b*-*p*PEK should be inherent to the chromophoric inner HPBO cores, which were shielded by the outer linear PEK shells. The morphology study suggested that both proton conductivity and optical behaviors of HPBO might be greatly influenced by the globular core−shell architecture.

Introduction

Fused aromatic−heterocyclic polymers such as polybenzoxazoles (PBO), polybenzothiazoles (PBT), and polybenzimidazoles (PBI) continue to attract R & D interest mainly because of their high-temperature capabilities as well as their attractive mechanical, optical, and electronic properties,[1,2] more recently because of their potential for high-temperature fuel cell applications.[3] However, they have limited processability due to their insoluble nature and high softening temperature, which is generally above their degradation temperature. Structural modification on these materials has been necessary to improve their processability and specific property requirements. The traditional, linear structures of fused aromatic−heterocyclic polymers have been well studied for decades; arguably, the enhancement in their structural[4] and optoelectronic[5] properties has almost plateaued. Thus, the requirements of next-generation materials are driving the need to improve solubility for the better processability, and the consideration of three-dimensional structures as an alternative strategy to specific properties, which could not be fulfilled by traditional aromatic−heterocyclic rigid-rod polymers. For these combined requirements, materials with dendritic structures such as dendrimers and hyperbranched polymers have a great potential in the development of future materials.[6] Although there are numerous publications on dendrimers and hyperbranched polymers for the past 20 years or so,[6b] the reports on the syntheses and characterization of fused aromatic−heterocyclic dendritic polymers are fairly rare.[7] As an initial entry into this area, a novel hyperbranched polymer containing alternating quinoxaline and benzoxazole repeat units was prepared via an aromatic−heterocyclic-forming reaction in poly(phosphoric acid) (PPA).[8]

Herein we report the design and synthesis of a new AB_2 monomer containing reactive moieties to engage in benzoxazole-forming reaction in PPA to generate an all-aromatic hyperbranched polybenzoxazole (HPBO), which was used as the core block for star-branched block copolymers synthesized in the same medium with additional optimized amount of phosphorus pentoxide (P_2O_5). The characterization of resultant star-block polymers was also investigated, and the results are reported here as well.

Experimental Section

Materials. All chemicals and solvents including poly(phosphoric acid) (PPA, assay ≥83% P_2O_5 content) and phosphorus pentoxide (P_2O_5) were purchased from Aldrich Chemical Inc. and used as received, unless otherwise specified. The AB monomers, 3- and 4-phenoxybenzoic acids for linear poly(ether ketone)s (PEK), were purchased from Aldrich Chemical Co. They were purified by recrystallization from toluene/heptane (5/5, v/v) mixture to give shiny colorless needles (mp 147−148.5 and 162−164 °C, respectively).[9]

Instrumentation. Elemental analysis and mass spectral analysis were performed by System Support Branch, Materials & Manufacturing Directorate, Air Force Research Laboratory, Dayton, OH. The melting points (mp) of all compounds were determined on a Mel-Temp melting point apparatus and are uncorrected. Intrinsic viscosities were determined using Cannon-Ubbelohde No. 200 viscometer. Flow times were recorded for methanesulfonic acid (MSA) solution, and polymer concentrations were in the range of 0.5−0.1 g/dL at 30.0 ± 0.1 °C. Differential scanning calorimetry (DSC) was performed under a nitrogen atmosphere with heating and cooling rates of 10 °C/min using a Perkin-Elmer DSC7 equipped with TAC7 controller. The DSC thermograms were obtained on powder samples after they had been heated to 400 °C and cooled to 20 °C. Glass transition temperatures (T_g's) were taken

* Corresponding authors: Tel +1-937-255-9153, Fax +1-937-656-6327, e-mail Loon-Seng.Tan@wpafb.af.mil (L.-S.T.); Tel +82-52-708-7034, Fax +82-52-708-7010, e-mail jbbaek@unist.ac.kr (J.-B.B.).
[†] Ulsan National Institute of Science and Technology.
[‡] Southwestern Ohio Council for Higher Education.
[§] Air Force Research Laboratory.

10.1021/ma802401v CCC: $40.75 © 2009 American Chemical Society
Published on Web 02/09/2009

as the midpoint of the baseline shift. Thermogravimetric analysis (TGA) was conducted both in air and nitrogen atmospheres with a heating rate of 10 °C/min using a Perkin-Elmer TGA7. Proton conductivity was evaluated using a two-point probe method with a Solartron 1260 ac impedance analyzer with an amplitude of 10 mV and a frequency range of 1−100 000 Hz at relative humidity of 50%. Each sample was fixed in a Teflon conductivity test cell consisting of a working and a reference Pt electrodes. The sample conductivity was determined by using $\sigma = (1/R)(L/A)$, where R is the resistance, L is the sample thickness, and A is the cross-sectional area. UV−vis spectra were obtained from a Perkin-Elmer Lambda 35 UV/vis spectrometer. Fluorescence studies were conducted with a Perkin-Elmer LS 55 fluorescence spectrometer. The applied excitation wavelength was the UV absorption maximum of each sample. The field emission scanning electron microscopy (FE-SEM) used in this work was LEO 1530FE. The energy-minimized structures were performed by the CS Chem3D Ultra computational package (version 8.0.3, CambridgeSoft Corp., Cambridge, MA 02140).

Dimethyl 4-Hydroxyisophthalate (1). Into a 250 mL three-necked round-bottom flask equipped with a magnetic stirrer, a condenser, and dropping funnel, a solution of 4-hydroxyisophthalic acid (15.0 g, 82.4 mmol) in 150 mL of dried methanol was charged. Freshly distilled thionyl chloride (75.0 g, 630.5 mmol) was then added dropwise for 30 min. The mixture was gently heated under reflux for 4 h. Upon cooling to room temperature, white flakes formed and were collected by suction filtration to give 16.3 g (94% yield); mp 93−94 °C. Anal. Calcd for $C_{10}H_{10}O_5$: C, 57.14%; H, 4.80%; O, 38.06%. Found: C, 56.89%; H, 4.72%; O, 38.15%. FT-IR (KBr, cm^{-1}): 3416, 3211, 2964, 1733, 1689. Mass spectrum (*m*/*e*): 210 (M^+, 100% relative abundance) 179, 151. ^{1}H NMR ($CDCl_3$; δ ppm): 3.90 (s, 3H, CH_3), 3.98 (s, 3H, CH_3), 6.98−7.01 (d, 1H, Ar), 8.08−8.12 (dd, 1H, Ar), 8.53−8.54 (d, 1H, Ar), 11.19 (s, 1H, OH). ^{13}C NMR ($CDCl_3$; δ ppm): 52.09, 52.61, 112.14, 117.78, 121.44, 132.47, 136.58, 165.09, 165.99, 170.10.

Dimethyl 4-Hydroxy-5-nitroisophthalate (2). Into a 250 mL three-necked round-bottom flask equipped with a magnetic stirrer, a condenser, and nitrogen inlet, dimethyl 4-hydroxyisophthalate (15.0 g, 71.4 mmol) was dissolved in acetic acid (150 mL). Nitric acid (10 mL) was then added dropwise. The mixture was warmed at 60 °C for 12 h. After cooling down, the mixture was poured into water. The light yellow precipitate was collected, air-dried, and recrystallized from ethanol to give 16.0 g (88% yield) of light yellow crystals; mp = 74.76 °C. Anal. Calcd for $C_{10}H_9NO_7$: C, 47.07%; H, 3.55%; N, 5.49%; O, 43.89%. Found: C, 47.75%; H, 4.01%; N, 5.44%; O, 43.51%: FT-IR (KBr, cm^{-1}): 3076, 2992, 1722, 1690. Mass spectrum (*m*/*e*): 255 (M^+, 100% relative abundance), 241, 237. ^{1}H NMR (DMSO-d_6; δ ppm): 3.89 (s, 3H, CH_3), 3.97 (s, 3H, CH_3), 8.46−8.47 (d, 1H, Ar), 8.55−8.56 (d, 1H, Ar). ^{13}C NMR ($CDCl_3$, δ ppm): 52.72, 53.38, 117.60, 120.19, 130.61, 135.31, 138.50, 156.13, 163.70, 166.87.

Dimethyl 5-Amino-4-hydroxyisophthalate (3). Into a 500 mL high-pressure bottle, dimethyl 4-hydroxy-5-nitroisophthalate (15.0 g, 58.8 mmol), palladium on activated carbon (10%, 1.0 g), and acetic acid (200 mL) were charged. The bottle was placed on the hydrogenation vessel. Hydrogen was charged and discharged five times and agitated at 60−65 psi for 24 h. After filtered through Celite 545 to remove catalyst, the solvent was removed on a rotavap. The orange residue was recrystallized from deoxygenated ethanol to give 12.1 g (91% yield) of brown needles; mp 161−163 °C, 205 °C (free amine, dec), 335 °C (hydrochloric acid salt, dec). Anal. Calcd for $C_{10}H_{11}NO_5$: C, 53.33%; H, 4.92%; N, 6.22%, O, 35.52%. Found: C, 53.40%; H, 4.88%; N, 5.92%, O, 35.57. FT-IR (KBr, cm^{-1}): 3484, 3384, 2966, 1707, 1668. Mass spectrum (*m*/*e*): 225 (M^+, 100% relative abundance), 193, 165, 162. ^{1}H NMR (DMSO-d_6; δ ppm): 3.91 (s, 3H, CH_3), 3.99 (s, 3H, CH_3), 8.20−8.22 (d, 1H, Ar), 8.29−8.30 (d, 1H, Ar), 9.90 (NH, and OH). ^{13}C NMR (DMSO-d_6; δ ppm): 52.63, 53.33, 114.02, 121.07, 123.06, 128.23, 129.45, 157.51, 165.63, 170.72.

5-Amino-4-hydroxyisophthalic Acid Hydrochloride (4). Into a 250 mL three-necked, round-bottom flask equipped with a magnetic stirrer, nitrogen inlet, and a condenser, dimethyl 5-amino-4-hydroxyisophthalate (11.0 g, 48.8 mmol) and concentrated hydrochloric acid (200 mL) were placed. The mixture was then heated under reflux with vigorous stirring until the solution became homogeneous. It took about 6 h. While the mixture was cooling down, white flakes formed and were collected by suction filtration and dried under the reduced pressure to give 7.1 g (74% yield) of off-white crystals; mp >300 °C (dec). Anal. Calcd for $C_8H_8ClNO_5$: C, 41.13%; H, 3.45%; Cl, 15.18%; N, 6.00%; O, 34.24%. Found: C, 40.81%; H, 3.40%; Cl, 15.26%; N, 5.56%; O, 33.50%. FT-IR (KBr, cm^{-1}): 1684 (carboxylic C═O), 2580, 2892 (COOH), 3406 (NH), 3396 (OH). Mass spectrum (*m*/*e*): 197 (M^+, 100% relative abundance). ^{1}H NMR (DMSO-d_6, δ ppm): 8.21−8.22 (d, 1H, Ar), 8.30−8.31 (d, 1H, Ar), 9.91 (broad s, COOH, NH, and OH). ^{13}C NMR (DMSO-d_6; δ ppm): 114.01, 121.01, 123.05, 128.26, 129.47, 157.52, 165.64, 170.74.

Hyperbranched Polybenzoxazole (HPBO, 5). Into a 250 mL resin flask equipped with a high-torque mechanical stirrer, nitrogen inlet, and outlet, PPA (60 g) was placed and stirred with dried nitrogen purging for 10 h. The monomer, 5-amino-4-hydroxyisophthalic acid hydrochloride (1.5 g, 6.4 mmol), was added, and the resulting mixture was dehydrochlorinated under reduced pressure (1 mmHg) at 60 °C for 24 h, 100 °C for 24 h, and 130 °C. Upon completion of the dehydrochlorination step, the mixture was gently heated to 160 °C for 4 h. When the temperature was approach 160 °C, the mixture became viscous. The mixture was further heated to ensure complete ring closure to 180 °C for 24 h. At the end of the reaction, water was added into the flask and poured into a Warring blender and the bundles chopped, collected by suction filtration, washed with diluted ammonium hydroxide and then Sohxlet-extracted with water for 3 days and methanol for 3 days, and finally dried under reduced pressure (1 mmHg) at 150 °C for 48 h to give 1.01 g (97.6% yield) of brown solids. An intrinsic viscosity of 0.42 dL/g (30 ± 0.1 °C in MSA) and 0.20 dL/g (30 ± 0.1 °C in NMP) were determined. Anal. Calcd for $C_8H_3NO_3$: C, 59.64%; H, 1.88%; N, 8.69%; O, 29.79%. Found: C, 53.86%; H, 2.73%; N, 7.65%; O, 33.74%.

Hyperbranched PBO-*block*-*m*PEK Star Block Copolymerization (6). Into a 100 mL resin flask equipped with a high-torque mechanical stirrer, nitrogen inlet and outlet, PBO **5** (0.10 g, 0.62 mmol) and PPA (20 g) were placed. The mixture was heated to 130 °C and stirred for 8 h until the mixture became homogeneous. The AB monomer, 3-phenoxybenzoic acid (1.0 g, 4.67 mmol), and P_2O_5 (5.0 g) were added. The temperature was maintained at 130 °C for 48 h. At the end of the reaction, water was added to the flask and poured into a Warring blender. After the polymer bundles had been chopped, collected by suction filtration, and washed with diluted ammonium hydroxide, it was Sohxlet extracted with water for 3 days and then methanol for 3 more days, and finally dried under reduced pressure (1 mmHg) at 150 °C for 48 h to give 1.00 g (98.4% yield) of deep purple solids. An intrinsic viscosity of 1.65 dL/g (MSA, 30 ± 0.1 °C) was determined. Anal. Calcd for $C_{12.41}H_{7.41}N_{0.12}O_{2.12}$: C, 77.23%; H, 3.85%; N, 1.02%; O, 17.89%. Found: C, 76.14%; H, 4.20%; N, 0.79%; O, 17.67%.

Hyperbranched PBO-*block*-*p*PEK Star Block Copolymerization (7). Into a 100 mL resin flask equipped with a high-torque mechanical stirrer, nitrogen inlet, and outlet, PBO **5** (0.10 g, 0.62 mmol) and PPA (20 g) were placed. The reaction conditions and work-up procedures were the same as those for **6** to give 0.98 g (96.5% yield) of light pink solids. An intrinsic viscosity of 0.55 dL/g (MSA, 30 ± 0.1 °C) was determined. Anal. Calcd for $C_{12.41}H_{7.41}N_{0.12}O_{2.12}$: C, 77.23%; H, 3.85%; N, 1.02%; O, 17.89%. Found: C, 77.04%; H, 4.01%; N, 0.88%; O, 17.72%.

Extraction of Free *m*PEK from HPBO-*b*-*m*PEK. *m*PEK is amorphous polymer, and it is readily soluble in methylene chloride (CH_2Cl_2), but HPBO-*b*-*m*PEK is not. Therefore, the purple powder sample of HPBO-*g*-*m*PEK (1.00 g) was dispersed in CH_2Cl_2 in a closed vial at room temperature for 24 h. The suspension was collected by filtration. It was repeatedly dispersed in fresh CH_2Cl_2 and collected by filtration until no sign of dark spot from filtrate (free *m*PEK in CH_2Cl_2) on a thin-layer chromatography (TLC) plate.

Scheme 1. Monomer Synthesis[a]

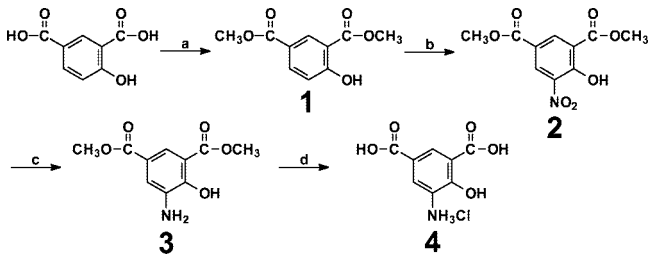

[a] a: $SOCl_2$/MeOH, reflux; b: HNO_3/AcOH, 60 °C; c: H_2 (65 psi), EtOH, rt; d: conc HCl, reflux.

The collected suspension was dried under reduced pressure (0.01 mmHg) to give 0.98 g of purple powder. The result indicated that the most of *m*PEK had been covalently attached onto HPBO.

Results and Discussion

AB_2 Monomer Synthesis. The AB_2 monomer for the hyperbranched benzoxazole parent polymer (HPBO), 5-amino-4-hydroxyisophthalic acid hydrochloride (**4**), was synthesized via a four-step sequence (Scheme 1). Thus, 4-hydroxyisophthalic acid was first converted to the corresponding bis(methyl ester), **1**, followed by nitration in glacial acetic acid to form the precursor, dimethyl 4-hydroxy-5-nitroisophthalate (**2**). Finally, the requisite AB_2 monomer was obtained in good yield after Pd/C-catalyzed hydrogen reduction of **2**, followed by treatment with concentrated HCl. All intermediates and the monomer were verified by conventional techniques such as melting point, proton and carbon nuclear magnetic resonance spectroscopy (^{1}H and ^{13}C NMR; see Supporting Information Figures S1a and S1b, respectively), Fourier-transform infrared spectroscopy (FT-IR), high-performance liquid chromatography (HPLC), and elemental and mass spectral analyses.

Polymerization of AB_2 Monomers. The polycondensation of the AB_2 monomer **4** to afford the parent polymer HPBO **5** was carried out at monomer concentration of 2.5 wt % and final reaction temperature at 180 °C in PPA (83% assay). We observed that soon after the reaction temperature had reached 160 °C, the mixture became very viscous, which was an indication of substantial molecular weight build-up. The mixture was further heated to 180 °C to ensure complete ring closure before work-up (Scheme 2). The final product was subjected to Soxhlet extraction with water for 3 days to completely remove residual PPA and methanol for an additional 3 days to remove any remaining low molecular mass impurities. The yield of product after complete work-up was almost quantitative, which was an indication of high conversion.

Star-Branched Block Copolymers. Because of the availability of large number of the carboxylic acid end groups of HPBO **5**, star-branched block copolymers could be prepared and utilized to tailor their physical properties for various applications. The average number of available reactive carboxylic acids on HPBO is equal to the degree of polymerization plus one (DP + 1), when the *o*-aminophenol focal point group is assumed to be intact. However, when the reactivity of functional group is high and the concentration of monomer is low (it was 2.5 wt % with reference to the amount of PPA used), the focal point would most likely react with one of peripheral carboxylic acids to form an intramolecular loop.[10] Hence, it is very likely that the number of available functional carboxylic acids on HPBO was equal to DP. By taking advantage of these reactive groups, polyarm-star block copolymers could be prepared by Friedel−Crafts acylation reaction using either 3- or 4-phenoxybenzoic acids as an AB monomer in the same pot with additional amount of phosphorus pentoxide (P_2O_5). The optimized reaction medium PPA/P_2O_5 can promote "direct" Friedel−Crafts acylation reaction, in which a carbocation ion ($-C^+{=}O \leftrightarrow -C{\equiv}O^+$, also known as acylium) could be generated directly from carboxylic acid instead of acid chloride as a polymer-forming reaction (Scheme 3).[11] Although one-pot syntheses of star block copolymers are possible by simply adding the corresponding monomers and additional P_2O_5 into the HPBO/PPA mixture right after homopolymerization, the parent polymer HPBO was isolated and completely worked up in this study in order to keep the molecular weight constant so that the resultant samples could be reasonably compared with each other. In this way, the isolated HPBO was redissolved in PPA, and then the corresponding AB monomer and the required amount of P_2O_5 was added. The resultant star block copolymers are denoted as HPBO-*b*-*m*PEK and HPBO-*b*-*p*PEK for HPBO-*block*-*meta*-poly(ether ketone) and HPBO-*block*-*p*-poly(ether ketone), respectively. The presence of free PEKs in the star block copolymers was indirectly determined by a simple extraction-and-weighing experiment on HPBO-*b*-*m*PEK (see Experimental Section for details). Considering possible loss during work-up routines, we estimated less than 2 wt % of free *m*PEK in the HPBO-*b*-*m*PEK. Thus, it could be assumed that most of PEKs were covalently linked to the HPBO.

Solution Properties. It has been established that hyperbranched polymers have generally higher solubility in a given solvent than their linear analogues with similar molecular weights.[12] Expectedly, the parent polymer HPBO **5** was found to be soluble in most of polar aprotic solvents (PAS) such as *N,N*-dimethylacetamide (DMAc), *N,N*-dimethylformamide (DMF), and *N*-methyl-2-pyrrolidinone (NMP), while its linear analogue, which is only soluble in strong acids such as sulfuric acid and methanesulfonic acid (MSA), is insoluble in these amide solvents.[13] However, we found that the extent of solubility of HPBO in PAS depended on the dryness of the sample. It was soluble in these solvents when the sample was not completely dry. Once the sample had been subjected to rigorous drying, it became much less soluble in PAS, but it could still dissolve quite well in strong acids such as trifluoroacetic acid (TFAA), sulfuric acid (MSA), and trifluoromethanesulfonic acid (TFMSA). While an in-depth investigation of this phenomenon was beyond the scope of this project, we could, however, theorize that the relationship between sample's solubility and dryness in common polar aprotic solvents is presumably due to the formation of strong intra- and intermolecular hydrogen bonding, which are driven by the large number of peripheral carboxylic acids. The proposed hydrogen-bonded structures are depicted in Scheme 4, and we offer a tentative explanation as follows. When the sample contains certain amount of water, the formation of intra- or intermolecular hydrogen bonding within a HPBO macromolecule or among a group of HPBO macromolecules, respectively, is hampered by water molecules (Scheme 4a), each of which can accept two hydrogen bonds and donate two hydrogen bonds as opposed to a COOH group, which can only accept a hydrogen bond and donate a hydrogen bond. For example, when its residual water content was more than 5 wt % by TGA, a HPBO sample was soluble in PAS, and there were no insoluble gels observed in the solutions. On the other hand, when the sample was completely dry (i.e., without water molecules act as some sort of plasticizer), intra- and intermolecular hydrogen bonding could be formed strongly among the HPBO macromolecules, which could be more tightly packed in a 3-dimensional fashion (Scheme 4b). As a result, completely dried HPBO showed limited solubility in PAS. To provide a proof for the above scenario, a HPBO sample was freeze-dried while it was still wet after Soxhlet extraction with water. The freeze-dried

Scheme 2. Synthesis of Hyperbranched Poly(Benzoxazole) (HPBO) 5 (Idealized Structure with *o*-Aminophenol as Focal Group and COOH as Terminal Groups)

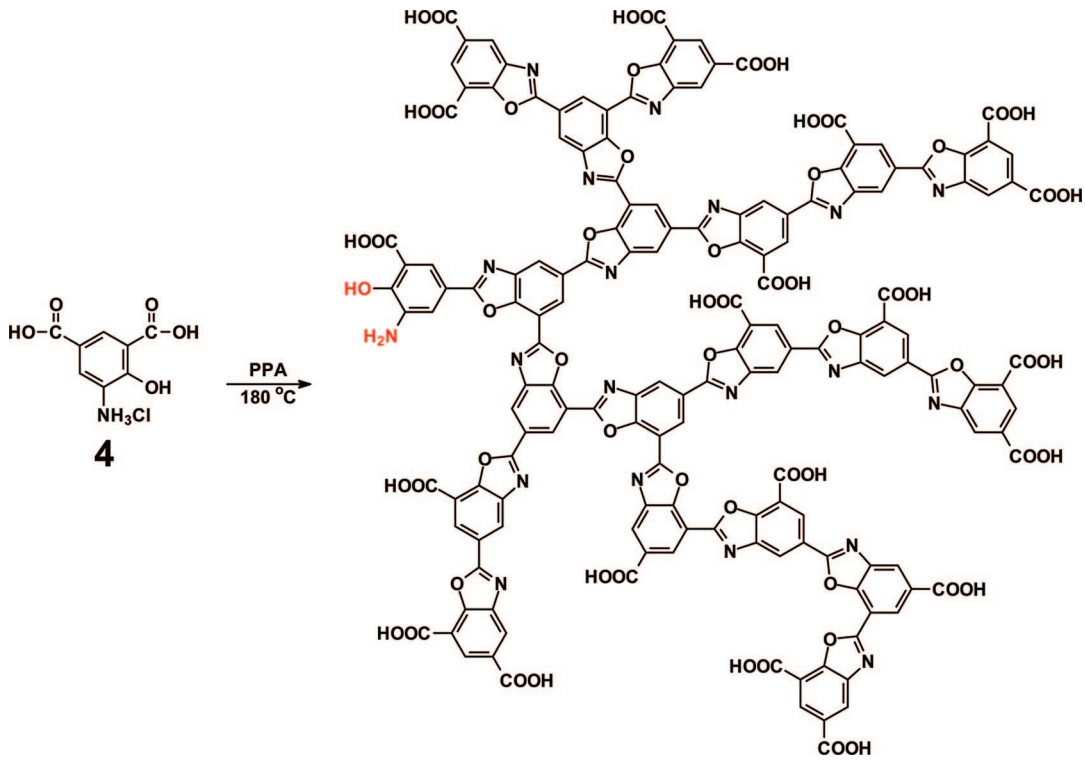

Scheme 3. Synthesis of Polyarm-Star Block Copolymers 6 and 7

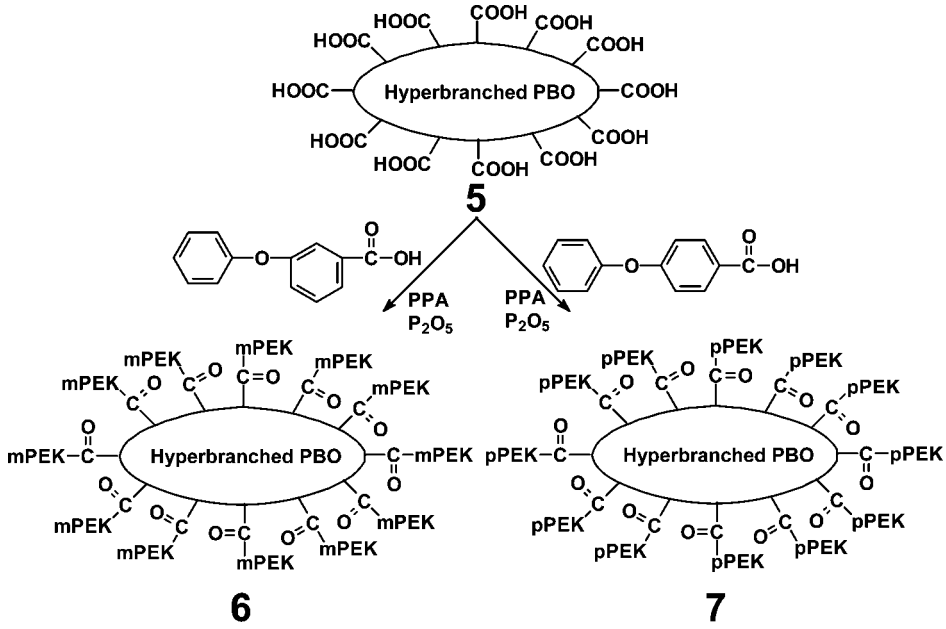

HPBO sample appeared to be much softer and fluffier, whereas another HPBO sample that had been dried in a vacuum oven under reduced pressure was rock hard. Furthermore, the freeze-dried sample was freely soluble in polar aprotic solvents. Thus, this empirical comparison together with the similar solubility behaviors that were observed and reported for the hydroxyl-terminated hyperbranched poly(phenylquinoxaline)[7a] and carboxylic acid-terminated hyperbranched poly(ether−ketone)s[10] could serve to buttress our explanation.

During the viscosity measurements, we observed that the HPBO parent polymer, which has numerous carboxylic acids on its periphery, displayed a strong polyelectrolyte behavior as a function of its concentration in both acidic (MSA) and basic (NMP) media (Figure 1). In the case of the HPBO in acidic solvent (MSA), both reduced and inherent viscosities were drastically increased. Since the carboxylic acids ($pK_a \sim 4.2$) on HPBO can act as proton acceptors in the presence of much stronger acid (in this case, MSA with a $pK_a \sim -2$), the resulting protonated HPBO became a polyelectrolyte (Scheme 5a). In the case of the HPBO sample in basic NMP solvent, the existence of polyelectrolyte effect is rather surprising because both NMP and carboxylic acid are not strong enough as a base and an acid to engage in a complete proton transfer process (i.e., salt formation). However, it is known that NMP can complex

Scheme 4. Schematic Representation of Proposed 3-D Hydrogen-Bonded Structures in HPBO: (a) Hydrated Sample; (b) Completely Dried Sample[a]

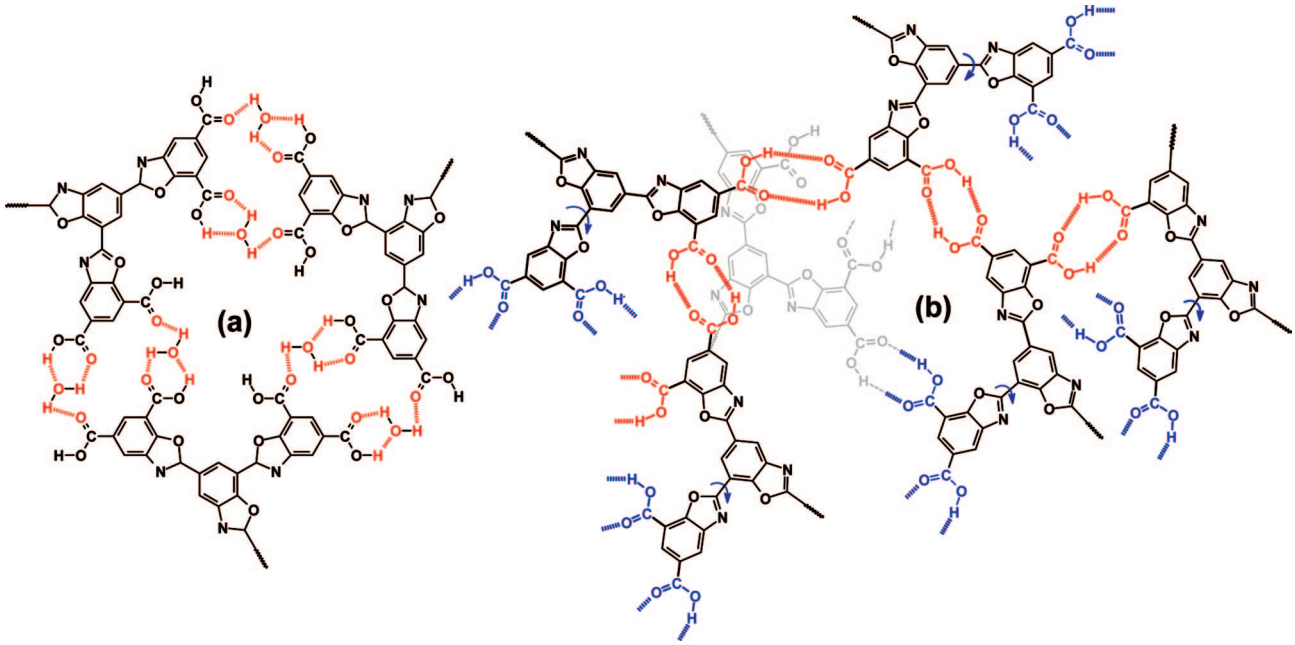

[a] The structural units shown in red are on the same plane while those shown in blue are out of the plane as a result of rotation around the C−C bond indicated by blue arrows.

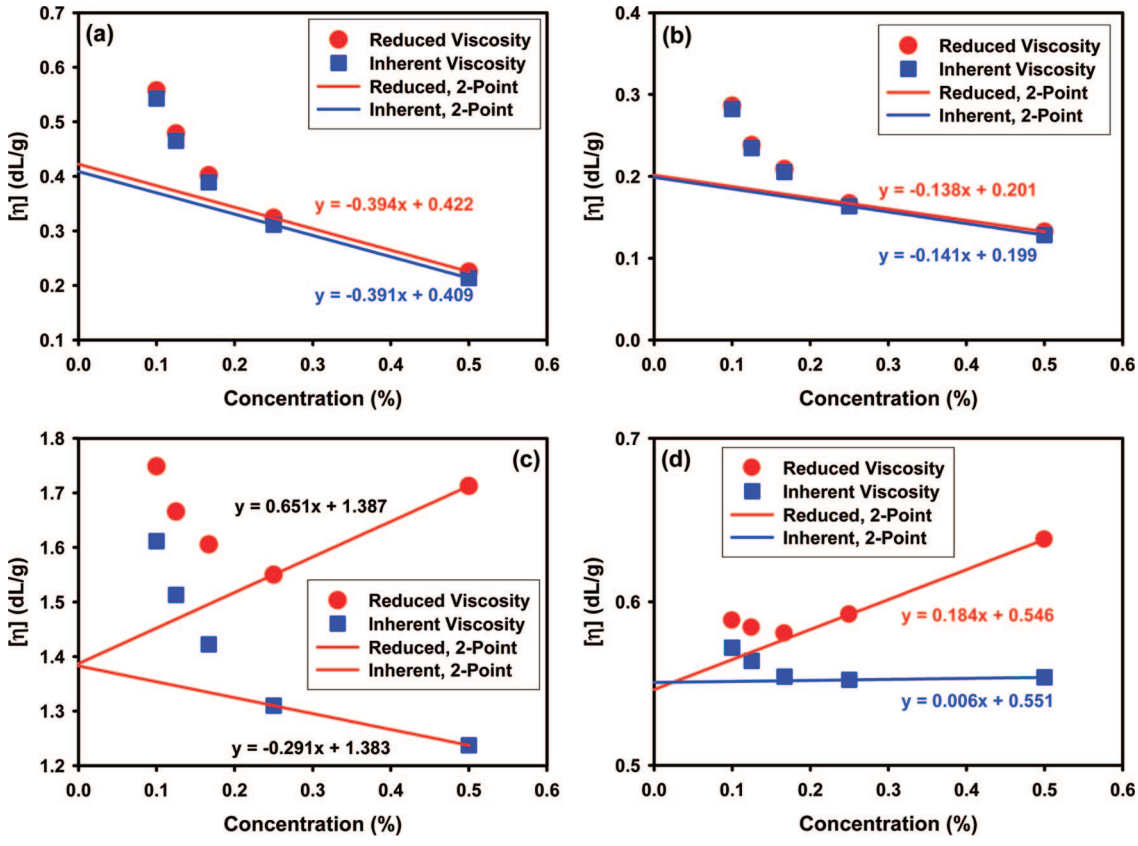

Figure 1. Solution behaviors of HPBO and its polyarm-star block copolymers: (a) HPBO in MSA; (b) HPBO in NMP; (c) HPBO-*g*-*m*PEK in MSA; (d) HPBO-*g*-*p*PEK in MSA.

strongly with an aromatic carboxylic acid via the combination of acid/base interaction and hydrogen bonding.[14] Such complexation (see Scheme 5b) is equilibrium-driven; i.e., the higher the NMP's number density (in other words, the more dilute HPBO concentration in NMP), the more complexes would form within each HPBO macromolecule, leading to more extended structure. Thus, we speculate that upon dilution HPBO macromolecules stretch out to greatly expand their hydrodynamic volumes, which results in the observed sharp increase in viscosity.

Scheme 5. Schematic Representation of Polyelectrolyte Structures: (a) Salt Formation in MSA Solution; (b) Proposed Complexation, Leading to Hydrodynamic Volume Expansion and Observed Polyelectrolyte Effect, in Dilute NMP Solution[a]

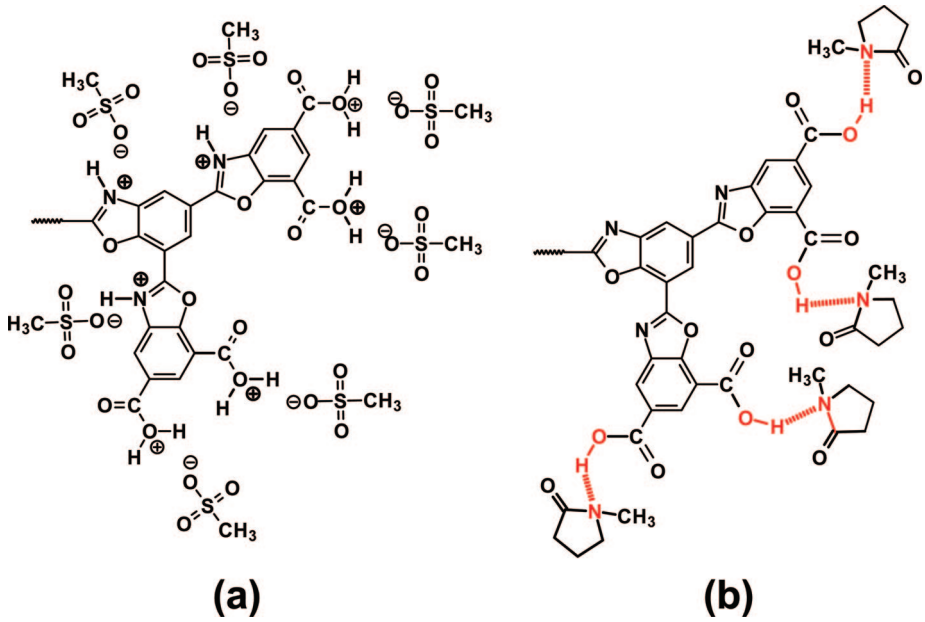

[a] Hydrogen bonds are highlighted in red.

Because of the polyelectrolyte effect, it was difficult to determine intrinsic viscosity ([η]) via the usual multipoint (five-point) measurement. Therefore, the approximate [η] values were obtained by extrapolating the initial two-point to zero concentration. HPBO had an intrinsic viscosity of 0.42 dL/g at 30 ± 0.1 °C in MSA solution and 0.20 dL/g at 30 ± 0.1 °C in NMP solution. The value obtained from the MSA solution is about 2 times higher than that obtained from the NMP solution. Furthermore, the slopes for the reduced and inherent viscosities are negative in both solutions. The latter result implies that the hydrodynamic volume of HPBO is getting larger as its concentration is lowered. With the caveat that the extrapolation to zero concentration might have overestimated the intrinsic viscosity values, this seems to suggest that in MSA solution the HPBO macromolecule is more "opened up" and chain-extended than when it is in NMP solution.

The star block copolymers, HPBO-*b*-*m*PEK and HPBO-*b*-*p*PEK, displayed much higher solution viscosities than the HPBO core due to the attachment of linear arms (Figure 1c,d). The copolymers had different reduced viscosity behavior compared to HPBO (Figure 1a). This implies that the molecular architecture of block copolymers has been changed. However, they still displayed polyelectrolyte effect because both block copolymers contained a large number of carboxylic acid chain ends. Another noteworthy point is that the viscosities of HPBO-*b*-*p*PEK (with stiffer *p*PEK chains) are lower than that of HPBO-*b*-*m*PEK (with more flexible *m*PEK chains). A plausible explanation for this otherwise surprising result is that the average molecular weight of *p*PEK chains could be significantly lower than that of *m*PEK as evidenced by our previous finding that the homopolymerization of 4-phenoxybenzoic acid and 3-phenoxybenzoic acid under the same conditions had led to *p*PEK with [η] = 0.69 dL/g and *m*PEK with [η] = 2.10 dL/g, respectively.[15] This is most likely because semicrystalline *p*PEK would start to fall out of the solution upon reaching certain molecular weight during polymerization.

Thermal Properties. HPBO is hygroscopic, stemming from the large number of carboxylic acids on its periphery and easily absorbs moisture even after having been dried under reduced pressure. Thus, it is not surprised that the outgassing of absorbed moisture featured prominently in the DSC thermogram of HPBO as a broad endotherm centered at 122 °C during the first heating scan (Figure 2a). Following immediately is another broad exotherm peaked around 223 °C, which would be attributed to the thermal relaxation of HPBO. It has been shown that the growing polymer molecules can store strain energy induced by viscosity and shear during polymerization in a viscous reaction medium such as PPA. Such stored strain energy would be released under appropriate thermal conditions.[15] The third endotherm was observed above 337 °C, assignable to the loss of carboxylic acids in the form of carbon dioxide. The glass transition temperature (T_g) was not detected in the range from room temperature to 400 °C in the second heating scan (Figure 2b). HPBO-*b*-*m*PEK displayed a T_g at 142 °C in the first heating scan, which was slightly increased to 144 °C during the second heating scan. Because *m*-poly(ether−ketone), *m*PEK, is an amorphous polymer, the HPBO-*b*-*m*PEK star block copolymer was also expected to be amorphous. The detected T_g value is ~7 °C higher than that of *m*PEK homopolymer (T_g = 137 °C) prepared under the same conditions.[11,15] This T_g increase could be because the rigid inner HPBO core was "holding" one end of each *m*PEK chain, restricting its mobility. In the case of HPBO-*b*-*p*PEK, it displayed melting endotherm peaked at 332 °C (heat of fusion, ΔH_f = 38 J/g) in the first heating scan (Figure 2a). This value is ~12 °C lower than that of *p*PEK homopolymer (T_m = 344 °C, ΔH_f = 33 J/g).[11,15] The melting point depression of HPBO-*b*-*p*PEK could be originated from the poorer chain mobility of *p*PEK from being tied to the rigid HPBO core. Hence, the *p*PEK chains in the star block copolymer should form less stable crystals (i.e., the degree of crystallinity is much reduced as compared to that of *p*PEK homopolymer). In the second heating scan (Figure 2b), HPBO-*b*-*p*PEK displayed T_g at 164 °C, which was comparable to that of *p*PEK homopolymer (T_g = 159 °C, first heating scan; T_g = 165 °C, second heating scan).[11,15] However, the T_m associated with a smaller endotherm detected during the second heating scan was 14 °C lower, at 318 °C, which might imply that the chain mobility of *p*PEK in HPBO-*b*-*p*PEK was also poorer, in addition to lower degree of crystallinity.

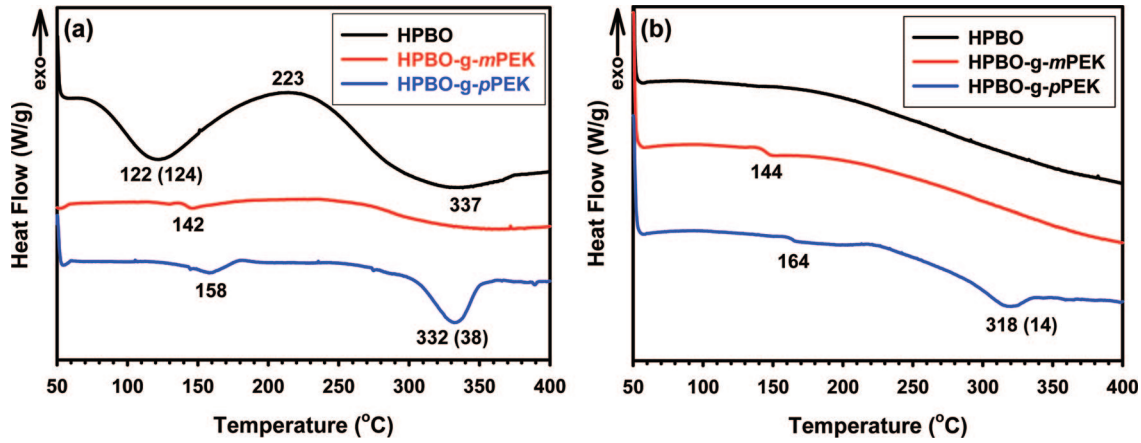

Figure 2. DSC thermograms of HPBO and its polyarm-star block copolymers: (a) first heating scan; (b) second heating scan.

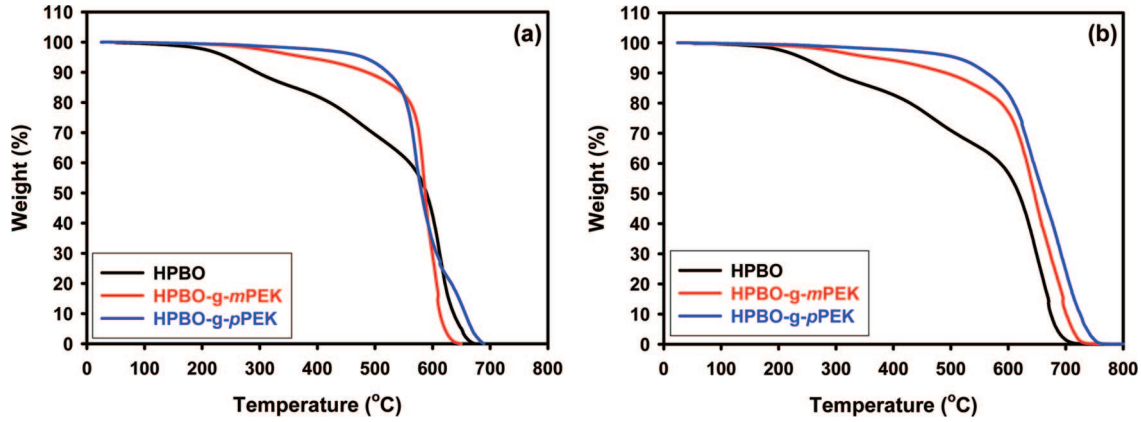

Figure 3. TGA thermograms of HPBO and its polyarm-star block copolymers: (a) in air; (b) in nitrogen.

Scheme 6. Idealized Structural Representation of Repeat Unit Segment in Two Liming Cases: (a) Fully Protonation of HPBO in MSA Solution; (b) Completely Neutral HPBO Structure in NMP Solution (See Scheme 5 Also)[a]

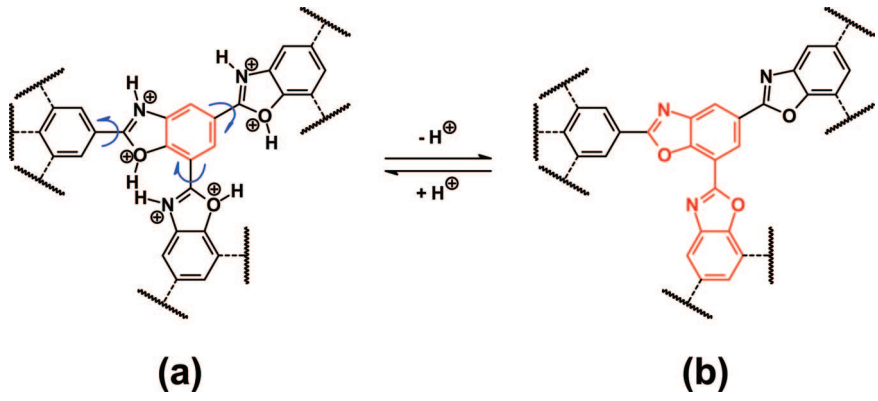

[a] In (a), the degrees of conjugation and aromaticity (shown in red) are reduced because of protonation and rotation around the C−C bonds (indicated by the blue arrows).

Thermo-oxidative and thermal stabilities of HPBO, HPBO-*b*-*m*PEK, and HPBO-*b*-*p*PEK were determined by thermogravimetric analysis (TGA). Since all the terminal groups (total number ~DP) of HPBO were hygroscopic carboxylic acids, HPBO displayed a stepwise weight-loss profile (Figure 3a). The early weight loss started around 200 °C when absorbed moisture outgassed. The discrepancy between the theoretical and experimental carbon numbers in the elemental analysis result (see Experimental Section) could be explained by this moisture uptake. The next weight loss around 380 °C was associated with the decomposition of carboxylic acid into carbon dioxide, which was also observed in a DSC study (see Figure 2a). The observed temperature for thermal CO_2 release agreed well with a previous study on the solid-state decomposition of benzoic acid derivatives.[16] The amount of carbon dioxide loss is ~27.0 wt %, which is in excellent agreement with the calculated value of 27.3 wt %.

The HPBO-*b*-*m*PEK and HPBO-*b*-*p*PEK samples were expected to be less hygroscopic because the number density of carboxylic acid groups in the star-block copolymer system is made smaller by the additional PEK repeat units. Hence, the TGA thermograms of both HPBO-*b*-*m*PEK and HPBO-*b*-*p*PEK do not show the early weight loss around 200 °C (Figure 3a). The 5 wt % weight loss temperatures ($T_{d5\%}$'s) of HPBO-*b*-*m*PEK

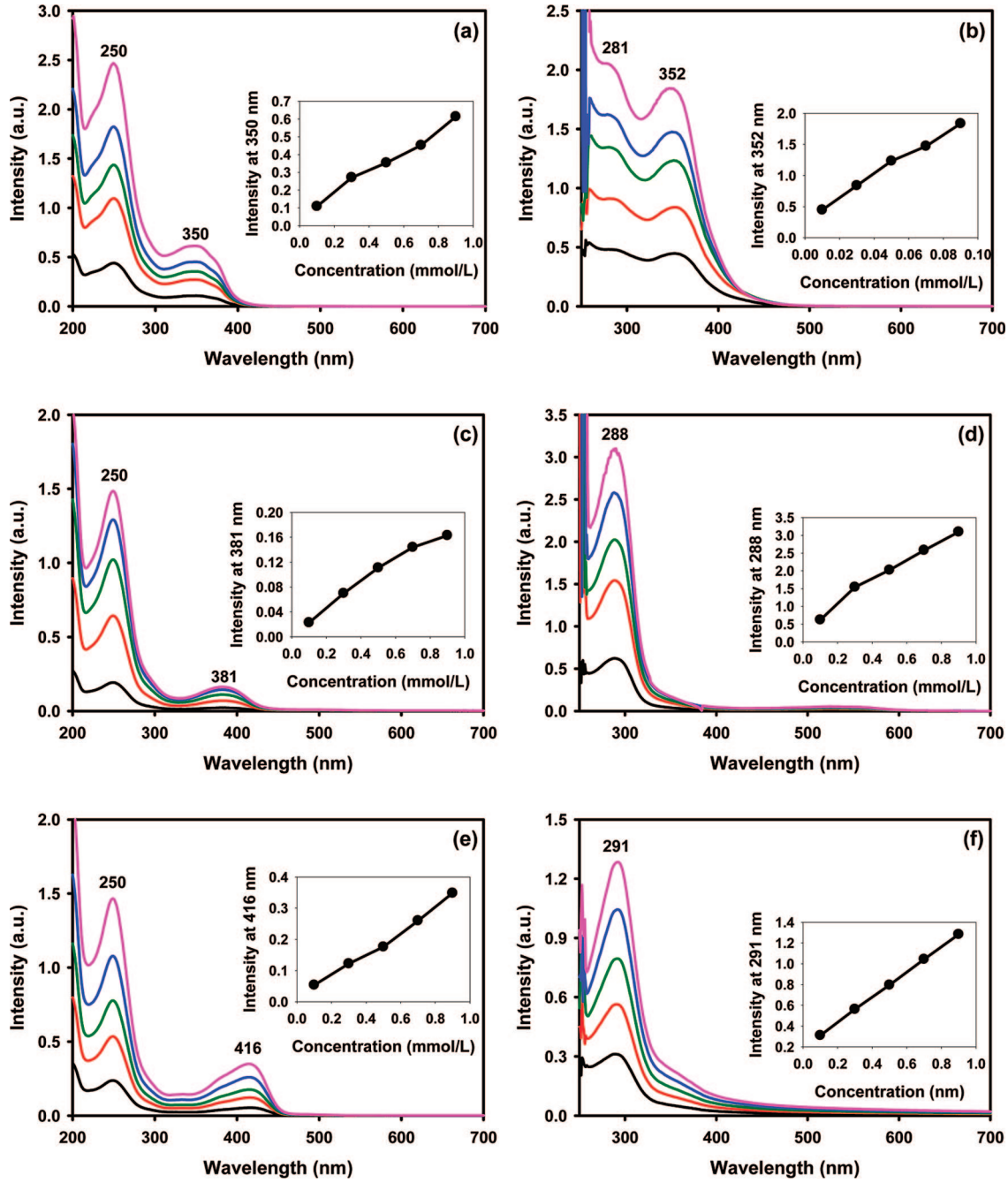

Figure 4. UV-absorption spectra of sample solutions: (a) HPBO in MSA; (b) HPBO in NMP; (c) HPBO-*g*-*m*PEK in MSA; (d) HPBO-*g*-*m*PEK in NMP; (e) HPBO-*g*-*p*PEK in MSA; (f) HPBO-*g*-*p*PEK in NMP.

and HPBO-*b*-*p*PEK were 380 and 480 °C in air, respectively. The $T_{d5\%}$'s of the samples in nitrogen were 368 and 510 °C, respectively (Figure 3b).

Optical Properties of HPBO. Since the linear analogues of HPBO, in particular rodlike poly(benzobisoxazole)s, are highly conjugated and therefore optically and electronically active,[17] it would be of special interest to assess how the hyperbranched architecture and the surface carboxylic groups influence HPBO's optical properties. Thus, the UV−vis absorption and fluorescence measurements of HPBO were conducted in both acidic MSA and basic NMP solutions. HPBO in acidic MSA solution displayed two strong absorption peaks in the UV region at 250 nm and the visible region at 350 nm (Figure 4a). HPBO in basic NMP solution showed those peaks at 281 and 352 nm, respectively (Figure 4b). In considering the environment effect, the wavelength values for the peaks in near-visible region were comparable, but for those in near-UV region there is a 31 nm span in the wavelength values between acidic and basic solutions. In addition, the intensity for the 250 nm peak is higher than that for the 350 nm peak in MSA, but the reverse is observed for the 281 and 352 nm peak in NMP. Furthermore, the intensity for the 350 or 352 nm peak was almost linearly dependent on HPBO concentrations in both solutions (see insets for Figure 4a,b), indicating that there was basically no concentration effect in the ground-state absorption of HPBO. We rationalize these results in terms of how the extents of coplanarity and conjugation length are adversely affected when the environment becomes highly acidic that all the lone-pair electrons are protonated, effectively hampering the delocalization process among the benzoxazole units, as shown in Scheme 6.

In the case of HPBO-*b*-*m*PEK in MSA solution (Figure 4c), the absorption maximum in the near-UV region remained

Scheme 7. Proposed Structure (b) for the "Interphase" Segment for Either HPBO-*b*-*m*PEK or HPBO-*b*-*p*PEK Where in MSA Protonation at the Imidazole Nitrogen or the Carbonyl and Imidazole Oxygens Leads to Two Types of Hydrogen-Bonded Six-Membered Ring Structures; Ring Structures Increase the Extent of Molecular Planarity (Highlighted in Red) in Comparison with the Neutral State, Idealized in Structure (a), Where Free Rotation around the C−C Bonds Indicated by Blue Arrows Would Disrupt Coplanarity of the Adjacent Benzoxazole Units

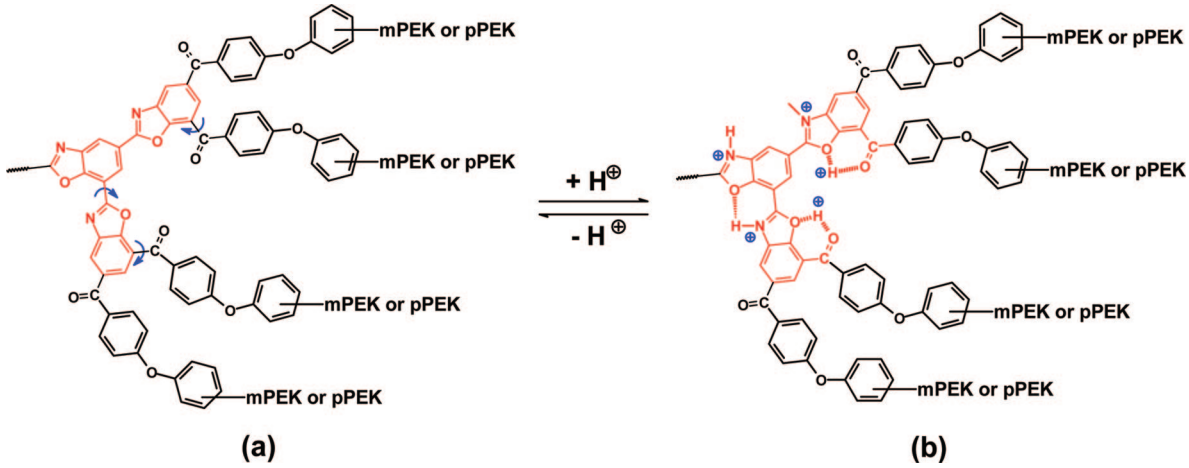

unchanged with respect to that of HPBO, but that in the near-visible region was red-shifted from 350 to 381 nm (Δ = 31 nm). However, in the NMP solution (Figure 4d), the near-visible absorption band of HPBO had practically vanished, while the near-UV absorption peak was slightly red-shifted from 281 to 288 nm (Δ = 7 nm).

In replacing *m*PEK with *p*PEK in the star block copolymer, we observed that the near-visible absorption band in MSA solution was red-shifted from 350 to 416 nm (Δ = 66 nm) in the visible region, while the near-UV absorption at 250 nm remained intact (Figure 4e). In switching from MSA to NMP, we found that the near-UV absorption was red-shifted from 281 to 291 nm (Δ = 10 nm). Similar to HPBO-*b*-*m*PEK in NMP, the near-visible band of HPBO at 352 nm had reduced to being a "shoulder" to the 291 nm band (Figure 4f).

In interpreting these results, we assume that the chromophoric component of the star block copolymers is the structural segments at the "interphase" where the peripheral COOH groups had made covalent linkages with the PEK chains. The assumption is reasonable because this is the location where the structural difference between HPBO and the star block copolymers could occur. The progressive shift of absorption maxima of HPBO, HPBO-*b*-*m*PEK, and HPBO-*b*-*p*PEK in both MSA and NMP solutions could be related to the geometry or conformation of HPBO's chromophoric component at the "inter phase" that is sensitive to protonation and, perhaps, other unknown processes as well. A noteworthy inference from these results is that numerous attachments of *m*PEK or *p*PEK to HPBO appear to promote greater electronic delocalization (i.e., an increase in the effective conjugation length or molecular planarity or both) in acidic MSA solution, while such mechanism is not accessible in basic NMP solution. We speculate that such mechanism is driven by the ability of MSA to protonate all lone-pair electrons and the consequential intramolecular hydrogen bonding leading to higher degree of coplanarity between the adjacent chromophoric benzoxazole units (see Scheme 7). Apparently, the para−para catenation of *p*PEK appears to be able to exert more bathochromic influence than the *m*PEK's meta−para catenation, judging from the wavelength shift between HPBO-*g*-*p*PEK (Δ = 56 nm) and HPBO-*g*-*m*PEK (Δ = 31 nm) of the HPBO absorption band at 350 nm.

Emission maxima of HPBO in MSA solution were in the blue region at 408 and 432 nm (Figure 5a). The peak intensity almost linearly decreased as concentration was increased due to an excimer quenching, which is favored by higher chromophore concentrations. The HPBO/NMP solution showed emission peak at 461 nm, which was 53 nm red-shifted as compared to that in MSA solution (Figure 5b). In conjunction with the results from UV−vis absorption study, the result also supports that the conformation of HPBO changes in different solvent systems (See Scheme 6). The shift should be attributable to the protonation to carboxylic acids and oxazole units on HPBO in strong acidic MSA. As in the case of MSA solution, NMP solution also displayed a decreasing trend in the emission intensity as the HPBO concentration was increased.

In the case of HPBO-*b*-*m*PEK, the emission peak in MSA solution was at 447 nm, which was red-shifted by 39 nm as compared to the HPBO/MSA solution (Figure 5c). The intensity was much less influenced by concentration variation and slightly decreased as the HPBO-*b*-*m*PEK concentration was increased. This was because the star block copolymer's chromophoric units were well shielded by the *m*PEK shell. The NMP solution of had an emission peak at 591 nm, which was 144 and 130 nm red-shifted as compared to the HPBO-*b*-*m*PEK/MSA solution and HPBO/NMP solution, respectively (Figure 5d). This indicates that the structure and properties of HPBO-*b*-*m*PEK's excited state are different from that of HPBO and also sensitive to solvent that is capable of engaging in specific interactions, e.g., acid−base equilibrium. It was noteworthy that the peak intensity drastically diminished as the star block copolymer's concentration was increased up to 0.7 mmol/L (Figure 5d, inset). But it reverted back to reach the highest intensity at 0.9 mM, and the result was reproducible. The origin of this behavior is presently unknown, but the result seems to imply that there is some kind of changeover in the polymer conformational dynamics in this specific concentration range.

The HPBO-*b*-*p*PEK/MSA solution displayed emission peak at 472 nm, which was 25 nm red-shifted as compared to that of HPBO-*b*-*m*PEK/MSA solution. The intensity also remained almost constant. Thus, similar to the results from the UV−vis absorption studies discussed above, the fluorescence results suggest that the conformation of the HPBO core would be somehow dependent on which type of PEK polymer was attached. Furthermore, if using its UV absorption behavior as a guide, this star block copolymer in NMP solution was expected to show more red shift in its fluorescence. However, as it turned out, the HPBO-*b*-*p*PEK/NMP solution displayed an emission maximum at 452 nm but with low intensity. This is because

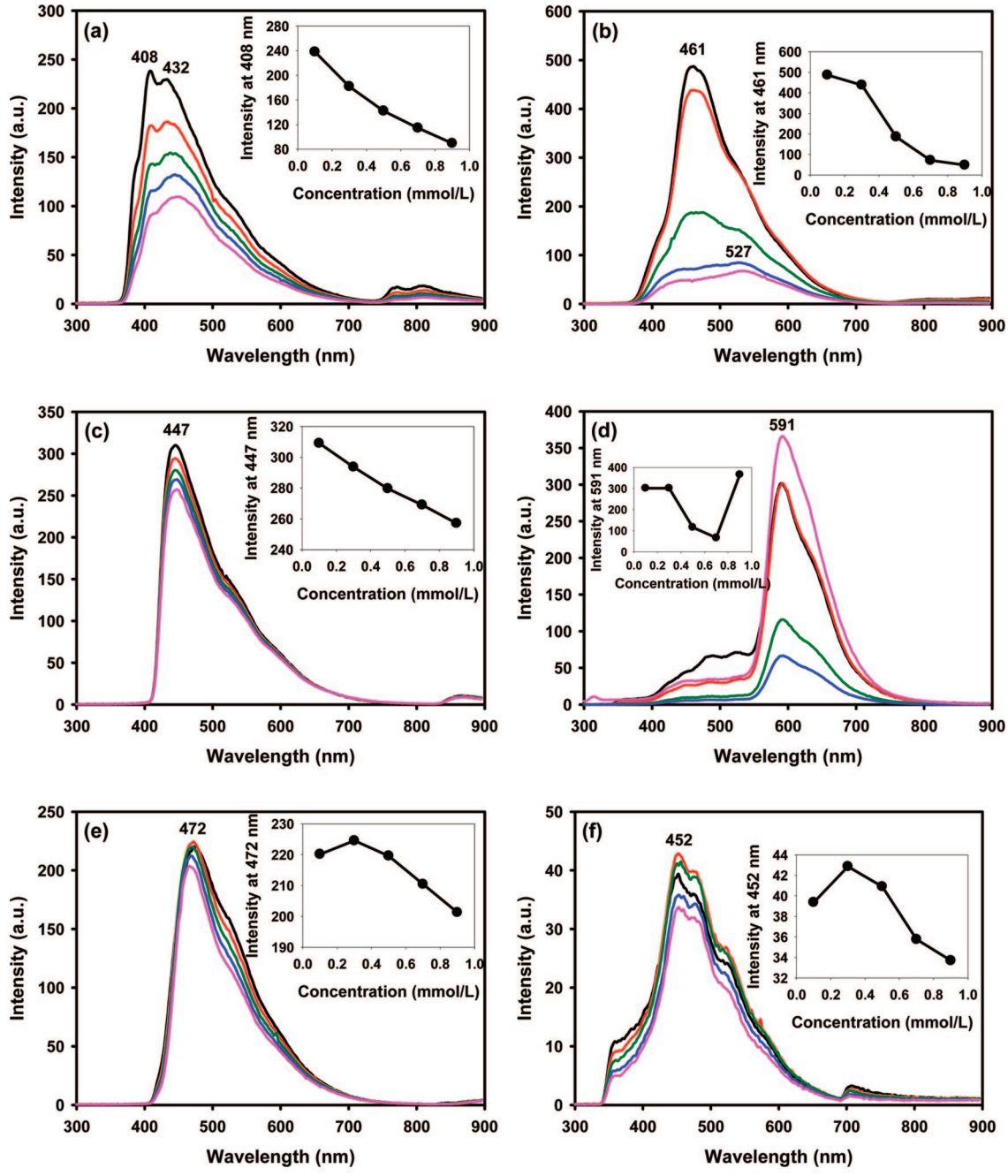

Figure 5. Fluorescence spectra of sample solutions: (a) HPBO in MSA; (b) HPBO in NMP; (c) HPBO-*g*-*m*PEK in MSA; (d) HPBO-*g*-*m*PEK in NMP; (e) HPBO-*g*-*p*PEK in MSA; (f) HPBO-*g*-*p*PEK in NMP.

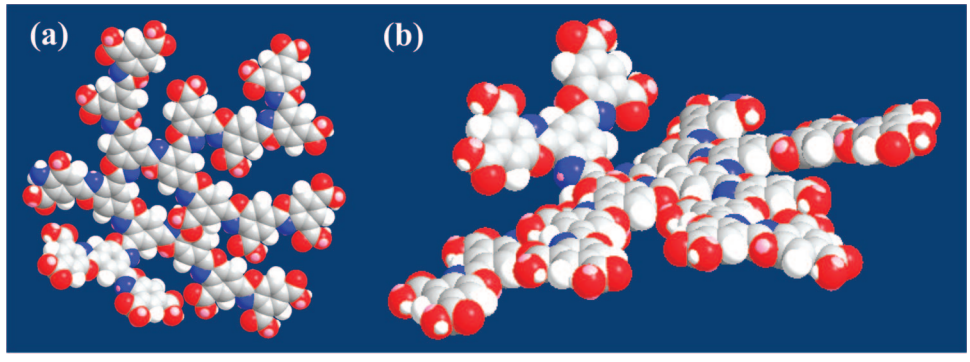

Figure 6. Energy-minimized space-filling structures of HPBO (CS Chem3D Ultra v8.0.3): (a) top view; (b) side view.

NMP is not a good solvent for semicrystalline *p*PEK.[18] Thus, the conformation of the star block copolymer must be in a greatly contracting mode in NMP, and thus, the HPBO's chromophoric units inside the block copolymers are being

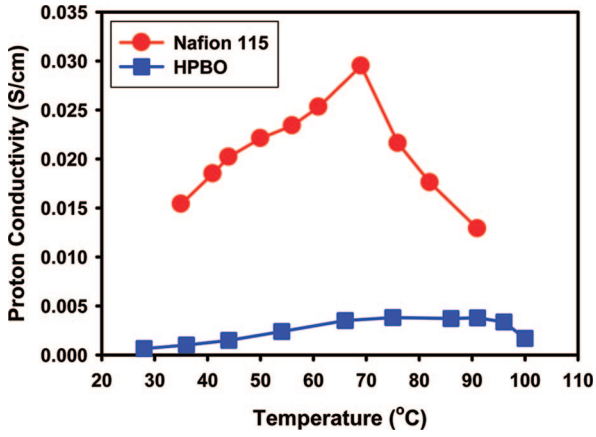

Figure 7. Proton conductivities of Nafion 115 and HPBO.

"squeezed" close to each other, promoting the intramolecular excimer quenching. In addition, the effective conjugation length/coplanarity of HPBO's chromophoric units in the block copolymer was also forced to be shorter than the chromophoric units in HPBO-*b*-*m*PEK.

On the basis of the results from the absorption and emission studies, it could be tentatively concluded that the protonation process in MSA significantly influences the excited state rather than the ground state of the chromophoric units located near the periphery of HPBO and at the "interphase" segment of the star block copolymers. However, while similar results with fluorescence Stokes shifts as a function of solvent polarity and the shielding effect of dendrimers[19] and dendrons[20] toward excimer quenching have been reported, the observed emission behaviors of our hyperbranched and star block systems are quite unique in a *strongly acidic* environment.

An energy-minimization computation study was conducted with a model HPBO molecule consisting of 20 repeating units. Although high molecular weight hyperbranched polymer is expected to have a globular architecture, an energy-minimized, space-filling molecular model shows that the structure of HPBO with 20 repeating units is quite planar (Figure 6). From this result, we could surmise that the degree of HPBO conjugation would be high enough to promote emitting light in the blue region as presented in the Figure 5.

Proton Conductivity of HPBO and Its Star Block Copolymers. Since there are numerous surface carboxylic acids present on the HPBO polymer, the proton conductivity was measured with two-point probe conductivity measurement at the relative humidity of 50% (Figure 7). For benchmarking, Nafion 115 was also evaluated under the same measuring conditions and found to display higher proton conductivity. However, the conductivity of Nafion 115 was dropping drastically when the temperature was raised above 70 °C. On the other hand, HPBO showed an initial value of 6.6×10^{-4} S/cm at 28 °C, which gradually increased as temperature was increased up to 90 °C before the decay started. Expectedly, the relatively lower proton conductivity of HPBO as compared to Nafion 115 could be explained in terms of their large acidity difference. The pK_a values of Nafion 115 and HPBO are ca. −6[21] and 4.2,[22] respectively. Thus, their pK_a difference is approximately ~10 to 11 orders of magnitude, but the difference in their proton conductivities is approximately an order of magnitude. It appears that in HPBO there is a nonlinear relationship between the acidity (at the molecular level) and proton conductivity (in the bulk state), and rather surprisingly at first, there is less temperature dependence in its proton conductivity. We suspect that the unique dendritic features of HPBO, namely (i) a large number of carboxylic acids per molecules and (ii) most of carboxylic acids would be present at the periphery of HPBO (see Figure 8b), may be the contributing factors. Further, since the dissociation of proton from carboxylic group is a function of temperature as opposed to the complete ionization of sulfonic group at room conditions (provided that enough water are present), it is reasonable to assume that the concentration of mobile protons in HPBO would increase with an increase in the surrounding temperature. Tentative explanations aside, this intriguing result has prompted us to further pursue a HPBO modified with sulfonic acid termini

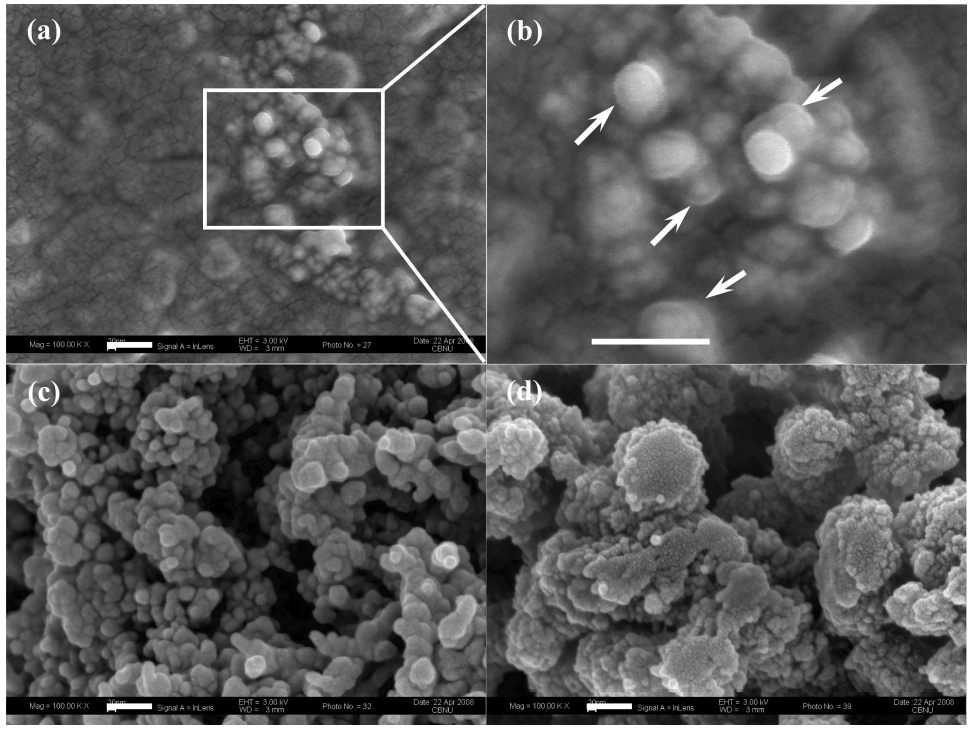

Figure 8. SEM images of samples: (a) HPBO (×100 000); (b) magnified image of (a); (c) HPBO-*g*-*m*PEK (×100 000); (d) HPBO-*g*-*p*PEK (×100 000). Scale bars are 100 nm.

to validate or refute our hypothesis. The synthesis and characterizations of such sulfonic acid-terminated HPBO are currently underway.

The proton conductivities of HPBO-*b*-*m*PEK and HPBO-*b*-*p*PEK were out of detection limit, since the number of carboxylic acids in copolymers was diluted by PEK units.

Scanning Electron Microscopy (SEM). The SEM images were obtained from powder samples. The morphology of HPBO appears to be made up of aggregating nanospheres (Figure 8a). Interestingly, these nanospheres could be discerned by two parts: a dense inner hard core is covered by fluffy outer shadow-like shell (Figure 8b, arrows). The diameters of the nanospheres are in the range of 10−40 nm. The inner hard part could be assigned to aromatic benzoxazole rings, and the fluffy outer shell could be mostly dominated by the carboxylic acids based on the fact that the electron density of inner aromatic benzoxazole rings is much higher than that of carboxylic acids. The SEM analysis visually supported the scenario in terms of the macromolecular architecture and surface chemistry at the molecular level to explain the higher than expected proton conductivity (see Figure 7) because of the relatively low acidity of the carboxylic acid and the observed optical behaviors of HPBO (see Figures 4 and 5).

The SEM image of HPBO-*b*-*m*PEK reveals that HPBO is well surrounded by *m*PEK (Figure 8c). The morphology is also dominated by the aggregations of nanospheres with diameter range of 10−40 nm. However, the interface between HPBO and *m*PEK could not be discerned since both are consisted of aromatic rings. The difference in the electron density between HPBO and *m*PEK may not be distinguishable. Thus, the morphology provides an indication that *m*PEK is grafted to the surface of HPBO. In the case of HPBO-*b*-*p*PEK (Figure 8d), the diameter dimension is much smaller than that of HPBO-*b*-*m*PEK apparently because *p*PEK is a semicrystalline polymer and, therefore, more compact. Overall, the particulate aggregates appear to be in much larger dimensions (>200 nm), while the individual particle dimension is 10−20 nm.

Conclusion

The AB_2 monomer, 5-amino-4-hydroxyisophthalic acid hydrochloride, was successfully synthesized and polymerized to afford high molecular weight hyperbranched polybenzoxazole (HPBO). The resultant HPBO was used as the core block for the subsequent synthesis of polyarm-star block copolymers. All the isolated polymers displayed polyelectrolyte behaviors in dilute solutions due to the presence of carboxylic acids on their peripheries. Specifically, since HPBO had the highest number of hydrophilic carboxylic acids per given weight, it clearly displayed stepwise weight-loss profile due to the bounded water and carboxylic acid decomposition. The UV−vis absorption behaviors for all samples with respect to the concentration were pseudo-linear dependence. However, the emission characteristics were significantly different between the HPBO parent polymer and the star block copolymers. While the emission intensity drastically decreased as the concentration of HPBO parent polymer was increased due to excimer quenching, the star-block copolymers were more or less unaffected by similar polymer concentration changes. This is apparently because in these star block copolymers the chromophoric units of the HPBO core were well protected from excimer quenching by their outer linear PEK shells in a good solvent. The unusual proton conductivity and emission behavior might have come from the morphology at the molecular level. The SEM image of HPBO showed that globular core−shell architecture of the HPBO in solid state. The high concentration of carboxylic acids on the surface of HPBO could be a reason why HPBO showed higher proton conductivity. While various hyperbranched polymers have been specifically synthesized for proton conductivity applications, as far as we know, the proton conductivities of these polymers are not based on carboxylic acid groups. Although the proton conductivity of our carboxylic acid-based hyperbranched polymer (HBPO) is still quite inferior, the observation that it is less temperature-dependent than Nafion provides some important insight for the design of improved high-temperature proton-conducting polymers.

Acknowledgment. We are grateful to Jeong Hee Lee (SEM) of Chungbuk National University and Dr. Yeong-Suk Choi (Proton Conductivity) of the Samsung Advanced Institute of Technology (SAIT) for obtaining data. This project was supported by funding from US Air Force Office of Scientific Research, Asian Office of Aerospace R&D (AFOSR-AOARD) and Korea Science and Engineering Foundation (R01-2007-000-10031-02).

Supporting Information Available: ^1H and ^{13}C NMR spectra of AB_2 monomer **4**, 5-amino-4-hydroxyisophthalic acid hydrochloride (Figure S1). This material is available free of charge via the Internet at http://pubs.acs.org.

Note Added After ASAP Publication. This article was published ASAP on February 9, 2009. In the thirteenth paragraph of the Results and Discussion section, a value for Δ has been changed. The correct version was published on February 12, 2009.

References and Notes

(1) (a) Zhou, C.; Wang, S.; Zhuang, Q.; Han, Z. *Carbon* **2008**, *46*, 1232. (b) Liu, Z.; Wang, S.; Zhuang, Q.; Li, X.; Li, F.; Wu, P.; Han, Z. *Chem. Mater.* **2007**, *19*, 1164. (c) Wang, S.; Chen, Y.; Zhuang, Q.; Li, X.; Wu, P.; Han, Z. *Macromol. Chem. Phys.* **2006**, *207*, 2336. (d) Wang, S.; Wu, P.; Han, Z. *J. Mater. Sci.* **2004**, *39*, 2717. (e) Tan, S. C.; Bai, Z.; Sun, H.; Mark, J. E.; Arnold, F. E.; Lee, C. Y. C. *J. Mater. Sci.* **2003**, *38*, 4013. (f) Cerruti, P.; Maglio, G.; Palumbo, R.; Tortora, M. *Macromol. Chem. Phys.* **2002**, *203*, 484. (g) Tan, L.-S.; Simko, S. R.; Bai, S. J.; Vaia, R. A.; Taylor, B. E.; Houtz, M. D.; Alexander, M. D., Jr.; Spry, R. J. *J. Polym. Sci., Part B: Polym. Phys.* **2001**, *39*, 2539.

(2) Reviews on polybenzobisazoles: (a) So, Y.-H. *Polym. Int.* **2006**, *55*, 127. (b) Huang, W.; Yin, J. *Polym. Bull.* **2006**, *57*, 269. (b) Lane, R. A. *AMPTIAC Q.* **2005**, *9* (2), 3. (c) Hu, X.-D.; Jenkins, S. E.; Min, B. G.; Polk, M. B.; Kumar, S. *Macromol. Mater. Eng.* **2003**, *288*, 823. (d) Sikkema, D. J.; Northolt, M. G.; Pourdeyhimi, B. *MRS Bull.* **2003**, *28*, 579. (e) Komarova, L. G.; Rusanov, A. L. *Russ. Chem. Rev.* **2001**, *70*, 81. (f) Adams, W. W., Eby, R. K., McLemore, D. E., Eds.; *The Materials Science and Engineering of Rigid-Rod Polymers*; MRS Symp. Proc. Vol. 134; Materials Research Society: Pittsburg, PA, 1989. (h) Wolfe, J. F. In *Encyclopedia of Polymer Science and Technology*, 2nd ed.; Mark, H. F., Kroschmitz, J. I., Eds.; Wiley: New York, 1988; Vol. 11, pp 601−635.

(3) (a) Li, Q.; Jensen, J. O. *Membr. Technol.* **2008**, *2*, 61. (b) Li, J.; Yu, H. *J. Polym. Sci., Part A: Polym. Chem.* **2007**, *45*, 2273. (c) Li, J.; Lee, C. H.; Park, H. B.; Lee, Y. M. *Macromol. Res.* **2006**, *14*, 438. (c) Lee, C. H.; Jung, C. H.; Lee, Y. M.; Rhim, J. W.; Nam, S. Y. *Desalination* **2006**, *200*, 664. (e) Harrison, W. L.; Hickner, M. A.; Kim, Y. S.; McGrath, J. E. *Fuel Cells* **2005**, *5*, 201.

(4) Reviews on structural applications: (a) Young, R. J.; Eichhorn, S. J. *Polymer* **2007**, *48*, 2. (b) Chae, H. G.; Kumar, S. *J. Appl. Polym. Sci.* **2006**, *100*, 791. (c) Northolt, M. G.; den Decker, P.; Picken, S. J.; Baltussen, J. J. M.; Schlatmann, R. *Adv. Polym. Sci.* **2005**, *178*, 1. (d) So, Y.-H. *Prog. Polym. Sci.* **2000**, *25*, 137. (e) Schartel, B.; Wendorff, J. H. *Polym. Eng. Sci.* **1999**, *39*, 128.

(5) Reviews on opto-electronic applications of rigid-rod polymers: (a) Kraft, A.; Grimsdale, A. C.; Holmes, A. B. *Angew. Chem., Int. Ed.* **1998**, *37*, 402, and references therein. (b) Alam, M. M.; Jenekhe, S. A. *Chem. Mater.* **2002**, *14*, 4775, and references therein For specific examples of all-aromatic rigid-rod polymers for LED applications, see: (c) Kanbara, T.; Inoue, T.; Sugiyama, K.; Yamamoto, T. *Synth. Met.* **1995**, *71*, 2207. (d) Thelakkat, M.; Schmidt, H.-W. *Polym. Adv. Technol.* **1998**, *9*, 429. (e) Bettenhausen, J.; Greczmiel, M.; Jandke, M.; Strohriegl, P. *Synth. Met.* **1997**, *91*, 223.

(6) For general reviews on dendritic macromolecules, see: (a) Gao, C.; Yan, D. *Prog. Polym. Sci.* **2004**, *29*, 183. (b) Jikei, M.; Kakimoto, M. *Prog. Polym. Sci.* **2001**, *26*, 1233. (c) Kim, Y. H. *J. Polym. Sci., Part A: Polym. Chem.* **1998**, *36*, 1685. (d) Hult, A.; Johansson, M.; Malmström, E. *Adv. Polym. Sci.* **1999**, *143*, 1. (e) Inoue, K. *Prog.*

Polym. Sci. 2000, *25*, 453. (f) Voit, B. *J. Polym. Sci., Part A: Polym. Chem.* **2000**, *36*, 2505. (g) Hult, A.; Malmström, E.; Johansson, M. In *Polymeric Materials Encyclopedia*; Salamone, J., Ed.; CRC Press: Boca Raton, FL, 1996; Vol. 5 H-L, p 3171.

(7) Aromatic heterocyclic hyperbranched polymers: (a) Baek, J.-B.; Harris, F. W. *Macromolecules* **2005**, *38*, 297. (b) Baek, J.-B.; Harris, F. W. *Macromolecules* **2005**, *38*, 1131. (c) Baek, J.-B.; Tan, L.-S. *Macromolecules* **2006**, *39*, 2794. (d) Gong, Z.-H.; Leu, C.-M.; Wu, F.-I.; Shu, C.-F. *Macromolecules* **2000**, *33*, 8527.

(8) Baek, J.-B.; Simko, S. R.; Tan, L.-S. *Macromolecules* **2006**, *39*, 7959.

(9) (a) Baek, J.-B.; Tan, L.-S. *Polym. Prepr.* **2002**, *43* (1), 533. (b) Baek, J.-B.; Tan, L.-S. *Polym. Prepr.* **2002**, *43* (1), 514.

(10) Choi, J.-Y.; Tan, L.-S.; Baek, J.-B. *Macromolecules* **2006**, *39*, 9057.

(11) Baek, J.-B.; Tan, L.-S. *Polymer* **2003**, *44*, 4135.

(12) For general reviews on hyperbranched polymers: (a) Fréchet, J. M. J. *Science* **1994**, *263*, 1710–1715. (b) Majoral, J. P.; Caminade, A. M. *Chem. Rev.* **1999**, *99*, 845–880. (c) Matthews, O. A.; Shipway, A. N.; Stoddart, J. F. *Prog. Polym. Sci.* **1998**, *23*, 1–56. (d) Bochkarev, M. N.; Katkova, M. A. *Russ. Chem. Rev.* **1995**, *64*, 1035–1048. (e) Tomalia, D. A.; Hedstrand, D. M.; Wilson, L. R. In *Encyclopedia of Polymer Science & Engineering*, 2nd ed.; Wiley and Sons: New York, 1990; p 46. (f) Burchard, W. *Adv. Polym. Sci.* **1983**, *48*, 1–124. (g) Turner, S. R.; Voit, B. I.; Mourey, T. H. *Macromolecules* **1993**, *26*, 4617–4623.

(13) Krause, S. J.; Haddock, T. B.; Vezie, D. L.; Lenhert, P. G.; Hwang, W. F.; Price, G. E.; Helminiak, T. E.; O'Brien, J. F.; Adams, W. W. *Polymer* **1988**, *29*, 1354.

(14) (a) Yu, J.; Ree, M.; Shin, T. J.; Wang, X.; Cai, W.; Zhou, D.; Lee, K. W. *J. Polym. Sci., Part B: Polym. Phys.* **1999**, *37*, 2806. (b) Kim, S. I.; Pyo, S. M.; Ree, M. *Macromolecules* **1997**, *30*, 7890. (c) Dauengauer, S. A.; Shibaev, L. A.; Sazanov, Y. N.; Stepanov, N. G.; Bulina, T. M. *J. Therm. Anal.* **1987**, *32*, 807.

(15) Baek, J.-B.; Park, S. Y.; Price, G. E.; Lyons, C. B.; Tan, L.-S. *Polymer* **2005**, *46*, 1543.

(16) Wesolowski, M.; Konarski, T. *J. Therm. Anal. Calorim.* **1999**, *55*, 995–1002.

(17) (a) *Handbook of Conducting Polymer*; Skotheim, T. A., Ed.; Marcel Dekker: New York, 1986, Vol. 2. (b) Burroughes, J. H.; Bradley, D. D. C.; Brown, A. R.; Marks, R. N.; Mackay, K.; Reiend, R. H.; Burns, P. L.; Holmes, A. B. *Nature (London)* **1990**, *347*, 539. (c) Osaheni, J. A.; Jenekhe, S. A. *Macromolecules* **1993**, *26*, 4726. (d) Jenekhe, S. A.; Osaheni, J. A. *Science* **1994**, *265*, 765.

(18) Bishop, M. T.; Karasz, F. E.; Russo, P. S.; Langley, K. H. *Macromolecules* **1985**, *18*, 86.

(19) Ceroni, P.; Bergamini, G.; Marchioni, F.; Balzani, V. *Prog. Polym. Sci.* **2005**, *30*, 453, and references therein.

(20) Wu, C.-W.; Sung, H.-H.; Lin, H.-C. *J. Polym. Sci., Part A: Polym. Chem.* **2006**, *44*, 6765, and references therein.

(21) (a) Kreuer, K. D. *J. Membr. Sci.* **2001**, *185*, 29. (b) Pathapati, P. R.; Xue, X.; Tang, J. *Renewable* **2004**, *30*, 1. (c) Ryder, A. G.; Power, S.; Glynn, T. *J. Appl. Spectrosc.* **2003**, *57*, 73.

(22) $pK_a = 4.19$ (25 °C). *The Merck Index*, 14th ed.; Merck & Co.: Whitehouse Station, NJ, 2006; p 180.

MA802401V